INTERNATIONAL STANDARD

ISO 14839-3

First edition
2006-09-15

Mechanical vibration — Vibration of rotating machinery equipped with active magnetic bearings —

Part 3: Evaluation of stability margin

Vibrations mécaniques — Vibrations de machines rotatives équipées de paliers magnétiques actifs —

Partie 3: Évaluation de la marge de stabilité

Reference number
ISO 14839-3:2006(E)

ISO copyright office
Case postale 56 • CH-1211 Geneva 20
Tel. + 41 22 749 01 11
Fax + 41 22 749 09 47
E-mail copyright@iso.org
Web www.iso.org

Published in Switzerland

Contents

Page

Foreword

ISO (the International Organization for Standardization) is a worldwide federation of national standards bodies (ISO member bodies). The work of preparing International Standards is normally carried out through ISO technical committees. Each member body interested in a subject for which a technical committee has been established has the right to be represented on that committee. International organizations, governmental and non-governmental, in liaison with ISO, also take part in the work. ISO collaborates closely with the International Electrotechnical Commission (IEC) on all matters of electrotechnical standardization.

International Standards are drafted in accordance with the rules given in the ISO/IEC Directives, Part 2.

The main task of technical committees is to prepare International Standards. Draft International Standards adopted by the technical committees are circulated to the member bodies for voting. Publication as an International Standard requires approval by at least 75 % of the member bodies casting a vote.

Attention is drawn to the possibility that some of the elements of this document may be the subject of patent rights. ISO shall not be held responsible for identifying any or all such patent rights.

ISO 14839-3 was prepared by Technical Committee ISO/TC 108, *Mechanical vibration and shock*, Subcommittee SC 2, *Measurement and evaluation of mechanical vibration and shock as applied to machines, vehicles and structures*.

ISO 14839 consists of the following parts, under the general title *Mechanical vibration — Vibration of rotating machinery equipped with active magnetic bearings*:

— Part 1: *Vocabulary*

— Part 2: *Evaluation of vibration*

— Part 3: *Evaluation of stability margin*

Additional parts are currently in preparation.

Introduction

While passive bearings, e.g. ball bearings or oil-film bearings, are essentially stable systems, magnetic bearings are inherently unstable due to the negative stiffness resulting from static magnetic forces. Therefore, a feedback control is required to provide positive stiffness and positive damping so that the active magnetic bearing (AMB) operates in a stable equilibrium to maintain the rotor at a centred position. A combination of electromagnets and a feedback control system is required to constitute an operable AMB system.

In addition to ISO 14839-2 on evaluation of vibration of the AMB rotor systems, evaluation of the stability and its margin is necessary for safe and reliable operation of the AMB rotor system; this evaluation is specified in this part of ISO 14839, the objectives of which are as follows:

a) to provide information on the stability margin for mutual understanding between vendors and users, mechanical engineers and electrical engineers, etc.;

b) to provide an evaluation method for the stability margin that can be useful in simplifying contract concerns, commission and maintenance;

c) to serve and collect industry consensus on the requirements of system stability as a design and operating guide for AMB equipped rotors.

Mechanical vibration — Vibration of rotating machinery equipped with active magnetic bearings —

Part 3: Evaluation of stability margin

1 Scope

This part of ISO 14839 establishes the stability requirements of rotating machinery equipped with active magnetic bearings (AMB). It specifies a particular index to evaluate the stability margin and delineates the measurement of this index.

It is applicable to industrial rotating machines operating at nominal power greater than 15 kW, and not limited by size or operational rated speed. It covers both rigid AMB rotors and flexible AMB rotors. Small-scale rotors, such as turbo molecular pumps, spindles, etc., are not addressed.

This part of ISO 14839 concerns the system stability measured during normal steady-state operation in-house and/or on-site.

The in-house evaluation is an absolute requirement for shipping of the equipment, while the execution of on-site evaluation depends upon mutual agreement between the purchaser and vendor.

This part of ISO 14839 does not address resonance vibration appearing when passing critical speeds. The regulation of resonance vibration at critical speeds is established in ISO 10814.

2 Normative references

The following referenced documents are indispensable for the application of this document. For dated references, only the edition cited applies. For undated references, the latest edition of the referenced document (including any amendments) applies.

ISO 10814, *Mechanical vibration — Susceptibility and sensitivity of machines to unbalance*

3 Preceding investigation

The AMB rotor should first be evaluated for damping and stability properties for all relevant operating modes. There are two parts to this assessment.

First, the run-up behaviour of the system should be evaluated based on modal sensitivities or amplification factors (Q-factors). This concerns all eigen frequencies that are within the rotational speed range of the rotor. These eigen frequencies are evaluated by the unbalance response curve around critical speeds measured in a rotation test.

When the unbalance vibration response is measured as shown in Figure 1, the sharpness of each vibration peak corresponding to eigen frequencies of the two rigid modes and the first bending mode is evaluated; this is commonly referred to as Q-factor evaluation. These damping (stability) requirements for an AMB system during run-up are covered by ISO 10814 (based on Q-factors), and are not the subject of this part of ISO 14839.

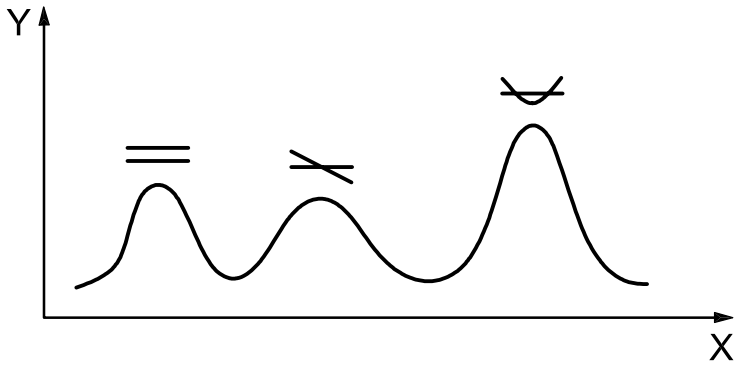

Key

X rotational speed

Y vibration magnitude

Figure 1 — Q-factor evaluation by unbalance vibration response

The second part, which is covered by this part of ISO 14839, deals with the stability of the system while in operation at nominal speed from the viewpoint of the AMB control. This analysis is critical since it calls for a minimum level of robustness with respect to system variations (e.g. gain variations due to sensor drifts caused by temperature variations) and disturbance forces acting on the rotor (e.g. unbalance forces and higher harmonic forces). To evaluate the stability margin, several analysis tools are available: gain margin, phase margin, Nyquist plot criteria, sensitivity function, etc.

4 Outline of feedback control systems

4.1 Open-loop and closed-loop transfer functions

Active magnetic bearings support a rotor without mechanical contact, as shown in Figure 2. AMBs are typically located near the two ends of the shaft and usually include adjacent displacement sensors and touch-down bearings. The position control axes are designated x_1, y_1 at side 1 and x_2, y_2 at side 2 in the radial directions and z in the thrust (axial) direction. In this manner, five-axis control is usually employed. An example of a control network for driving the AMB device is shown in Figure 3.

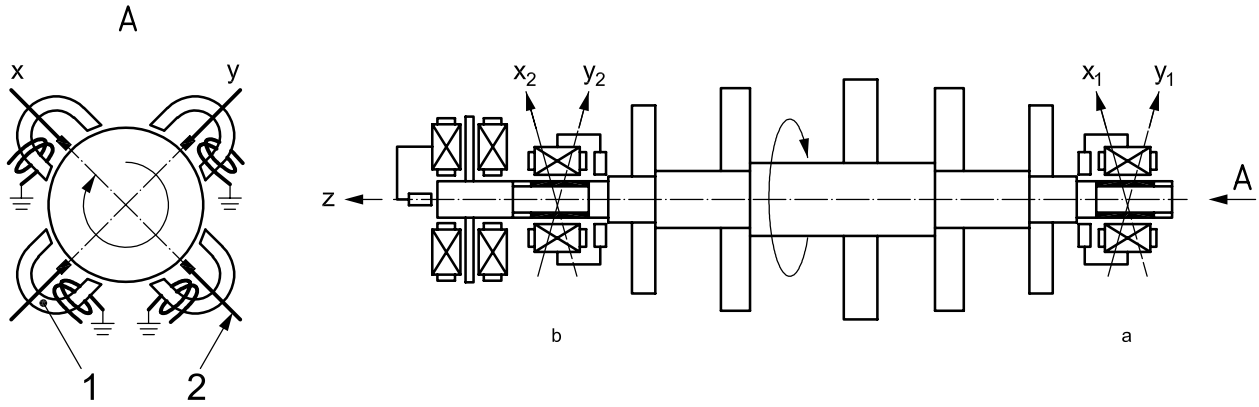

a) Axial view **b) Rotor system**

Key

1 AMB

2 sensor

a Side 1.

b Side 2.

Figure 2 — Rotor system equipped with active magnetic bearings

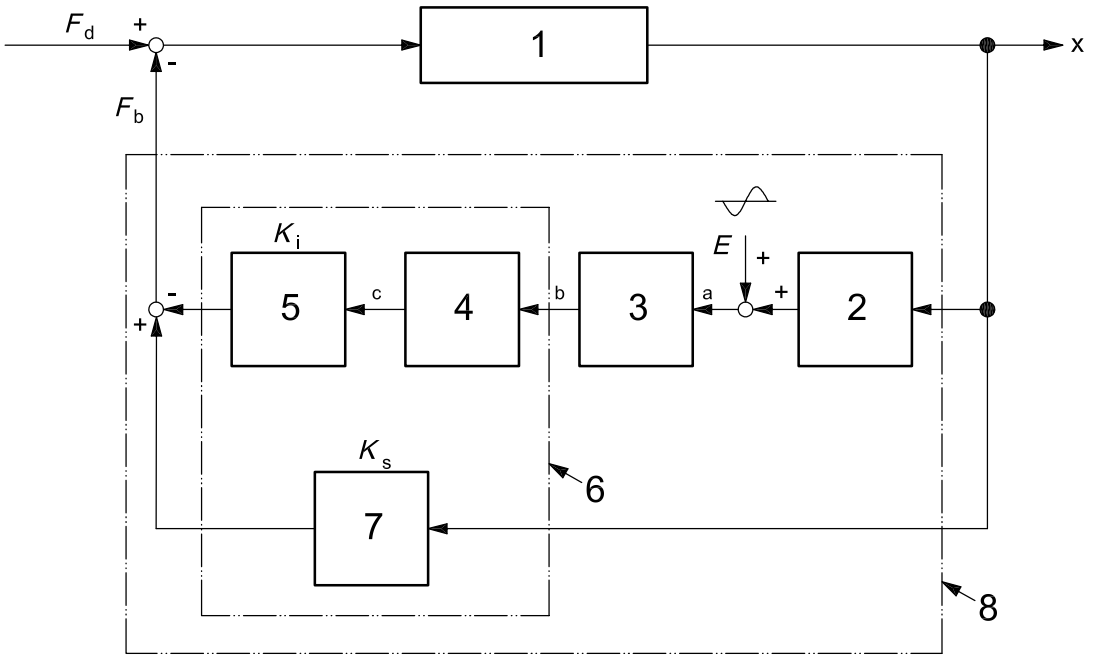

Key

1	mechanical plant rotor	E	excitation signal	a	Sensor signal.
2	position sensor, expressed in V/m	F_b	AMB force, expressed in newtons	b	Control signal.
3	AMB controller, expressed in V/V	F_d	disturbance force, expressed in newtons	c	Control current.
4	power amplifier, expressed in A/V	K_i	current stiffness, expressed in newtons per ampere		
5	electromagnet, expressed in N/A	K_s	negative position stiffness, expressed in newtons per metre		
6	AMB actuator	x	displacement, expressed in metres		
7	negative position stiffness, expressed in N/m				
8	AMB				

Figure 3 — Block diagram of an AMB system

As shown in these figures, each displacement sensor detects the shaft journal displacement in one radial direction in the vicinity of the bearing and its signal is fed back to the compensator. The deviation of the rotor position from the bearing centre is, therefore, reported to the AMB controller. The controller drives the power amplifiers to supply the coil current and to generate the magnetic force for levitation and vibration control. The AMB rotor system is generally described by a closed loop in this manner.

The closed loop of Figure 3 is simplified, as shown in Figure 4, using the notation of the transfer function, G_r, of the AMB control part and the transfer function, G_p, of the plant rotor. At a certain point of this closed-loop network, we can inject an excitation, $E(s)$, as harmonic or random signal and measure the response signals, V_1 and V_2, directly after and before the injection point, respectively. The ratio of these two signals in the frequency domain provides an open-loop transfer function, G_o, with $s = j\omega$, as shown in Equation (1):

$$G_o(s) = -\frac{V_2(s)}{V_1(s)} \tag{1}$$

Note that this definition of the open-loop transfer function is very specific. Most AMB systems have multiple feedback loops (associated with, typically, five axes of control) and testing is typically done with all loops closed. Consequently, the open-loop transfer function for a given control axis is defined by Equation (1) with the assumption that all feedback paths are closed when this measurement is made. This definition is different from the elements of a matrix open-loop transfer function defined with the assumption that all signal paths from the plant rotor to the controller are broken. See Annex E for a more detailed discussion of this issue.

The closed-loop transfer function, G_c, is measured by the ratio as shown in Equation (2):

$$G_c(s) = -\frac{V_2(s)}{E(s)} \tag{2}$$

The transfer functions of the closed loop, G_c, and open loop, G_o, are mutually consistent, as shown in Equations (3):

$$G_c = \frac{G_o}{1+G_o} \text{ and } G_o = \frac{G_c}{1-G_c} \tag{3}$$

The transfer functions, G_c and G_o, can typically be obtained using a two-channel FFT analyser. The measurement of G_o is shown in Figure 4 a).

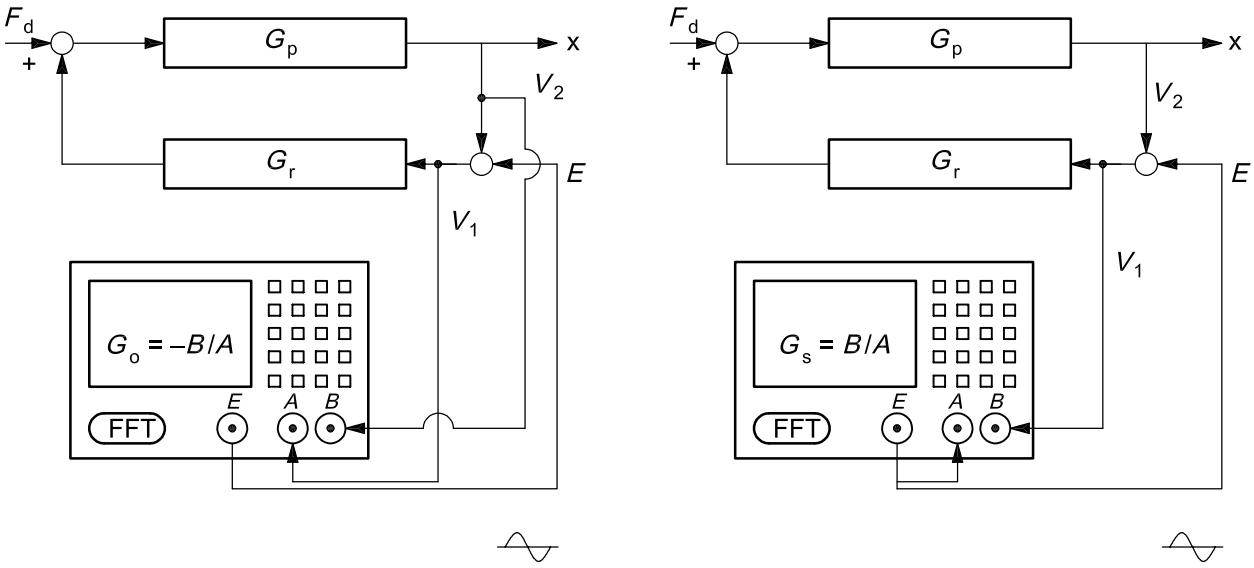

a) Measurement of G_o **b) Measurement of G_s**

Key

G_p transfer function of the plant rotor
G_r transfer function of the AMB control part
E external oscillation signal
G_o open-loop transfer function
G_s sensitivity function

Figure 4 — Two-channel measurement of G_o and G_s

4.2 Bode plot of the transfer functions

Once the open-loop transfer function, G_o, is measured as shown in Figure 5, we can modify it to the closed-loop transfer function, G_c, as shown in Figure 6. Assuming here that the rated (non-dimensional) speed is $N = 8$, the peaks of the gain curve at $\omega_1 = 1$, $\omega_2 = 6$ are distributed in the operational speed range so that the sharpness, i.e. Q-factor, of these critical speeds are regulated by ISO 10814. This part of ISO 14839 evaluates the stability margin of all of the resulting peaks, noted $\omega_1 = 1$, $\omega_2 = 6$ and $\omega_3 = 30$ in this example.

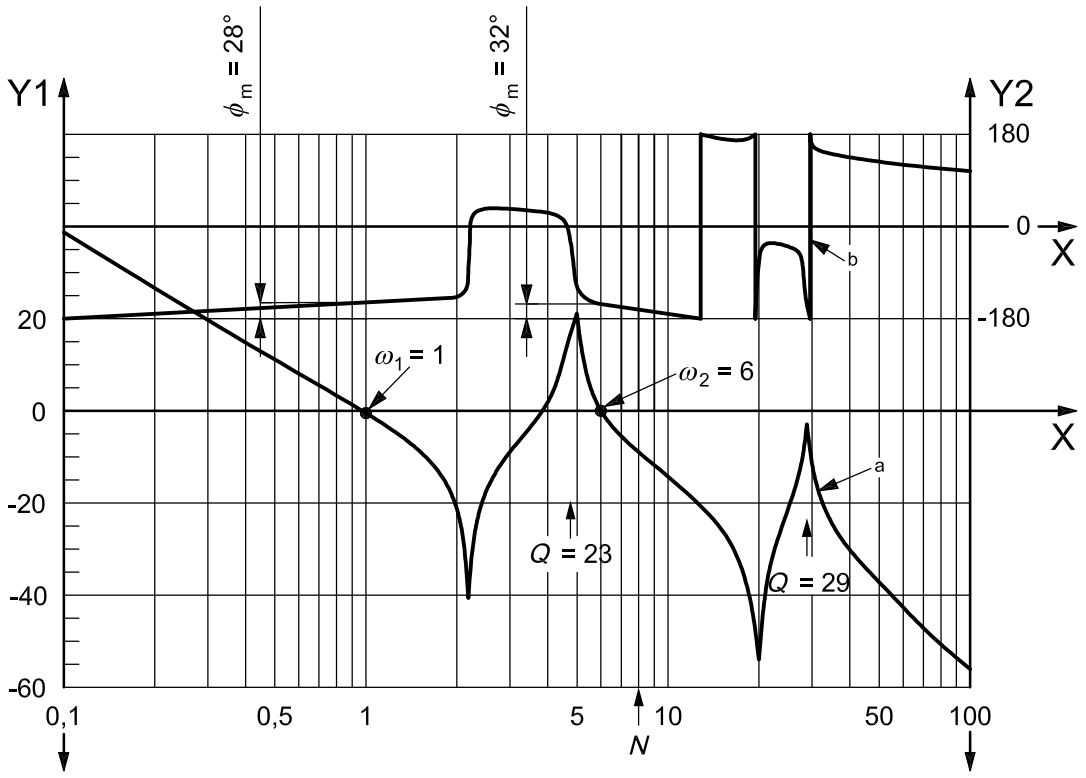

Key

X non-dimensional rotational speed

Y1 gain, expressed in decibels. The decibel (dB) scale is a relative measure: – 40 dB = 0,01; – 20 dB = 0,1; 0 dB = 1; 20 dB = 10; 40 dB = 100.

Y2 phase, ϕ, expressed in degrees

N rated non-dimensional speed

[a] Gain.

[b] Phase.

Figure 5 — Open-loop transfer function, G_o

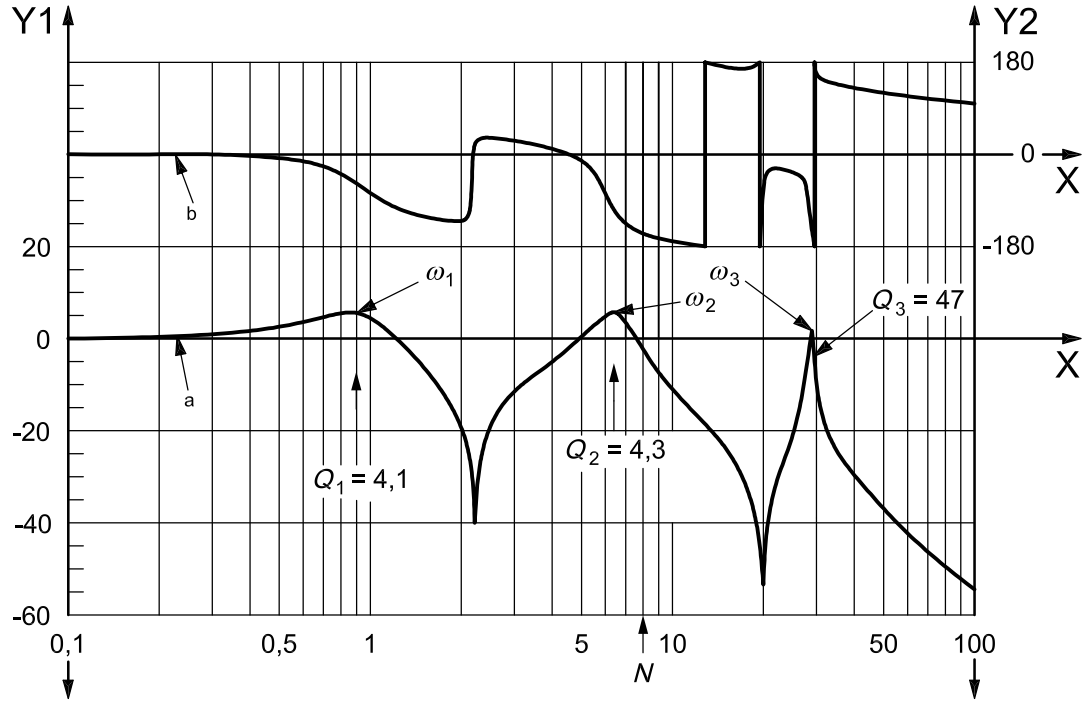

Key

X non-dimensional rotational speed

Y1 gain, expressed in decibels. The decibel (dB) scale is a relative measure: – 40 dB = 0,01; – 20 dB = 0,1; 0 dB = 1; 20 dB = 10; 40 dB = 100.

Y2 phase, ϕ, expressed in degrees

N rated non-dimensional speed

a Gain.

b Phase.

Figure 6 — Closed-loop transfer function, G_c

4.3 Nyquist plot of the open-loop transfer function

Besides the standard display in a Bode plot (see Figure 5), the open-loop transfer function $G_o(j\omega)$ can also be displayed on a polar diagram in the form of magnitude $|G_o(j\omega)|$ and phase of $G_o(j\omega)$ as shown in Figure 7 (note the dB polar diagram employed). Such a diagram is called the Nyquist plot of the open-loop transfer function. Since the characteristic equation is provided by $1 + G_o(s) = 0$, the distance between the Nyquist plot and the critical point A at (– 1, 0) is directly related to the damping of the closed-loop system and its relative stability. Generally, it can be stated that the larger the curve's minimum distance from the critical point, the greater is the system stability.

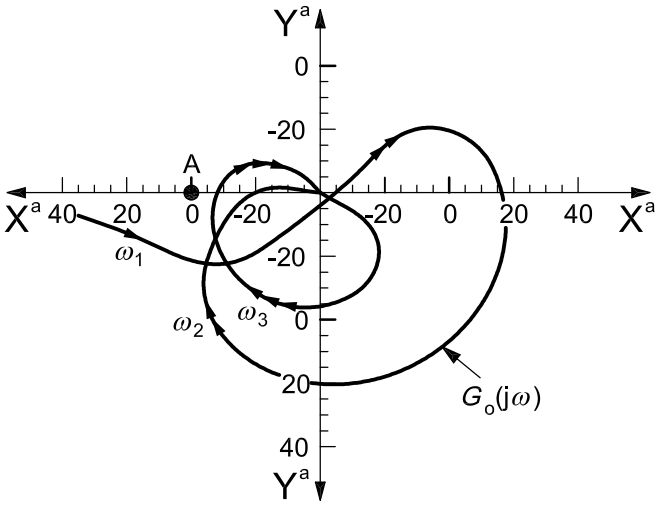

a) ω_1, ω_2 **and** ω_3

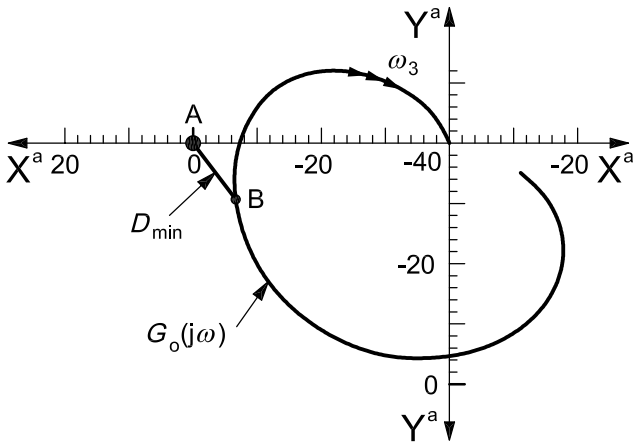

b) ω_3 **enlarged**

[a] The decibel (dB) scale is a relative measure: − 40 dB = 0,01; − 20 dB = 0,1; 0 dB = 1; 20 dB = 10; 40 dB = 100.

Figure 7 — Nyquist plot of the open-loop transfer function (dB polar diagram)

The enlargement of this Nyquist plot on a linear polar diagram is drawn in Figure 8, focusing on the critical point (–1, 0). The shortest distance measured from the critical point is indicated by $l_{AB} = D_{min}$, where a circle of radius D_{min} centred at (− 1, 0) is the tangent to the locus. For this example in Figure 8, the gain margin is the distance, l_{AG} (an intersection between the locus and the real axis), and the phase margin is the angle, ϕ, (between the real axis and a line extending from the origin to the intersection, P, between the locus and the unit circle centred on the origin). In this example, since $D_{min} < l_{AP}$ and $D_{min} < l_{AG}$, the shortest distance, D_{min}, is a more stringent evaluation criterion compared with the gain margin and the phase margin.

NOTE It can be shown that the shortest distance is always a more conservative measure of stability robustness than either gain or phase margin.

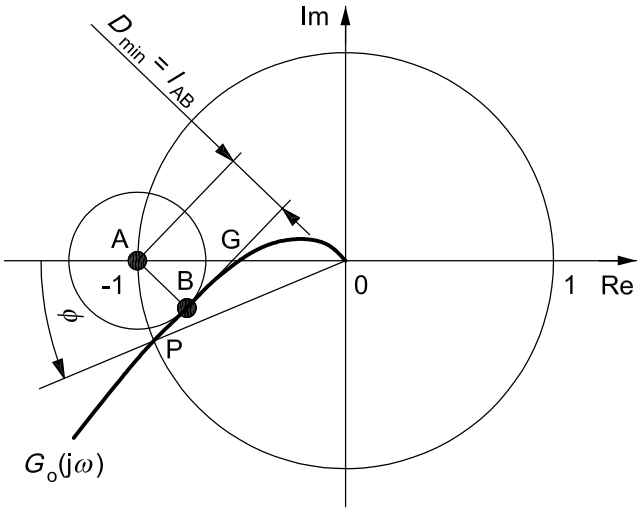

Figure 8 — Nyquist plot of the open-loop transfer function (linear polar diagram)

4.4 Sensitivity function

Note that, with the Nyquist plot, interest is focused on the distance between $G_o(j\omega)$ and the point (– 1, 0). That is, we want to know how small the value of $1 + G_o(j\omega)$ can be. Alternatively, one can ask how large the inverse of this function can be. If a small minimum value of $1 + G_o(j\omega)$ is undesirable, then so is a large maximum value of $1/[1 + G_o(j\omega)]$. This latter expression defines the sensitivity function G_s with $s = j\omega$, as shown in Equation (4):

$$G_s(s) = \frac{1}{1 + G_o(s)} \tag{4}$$

The maximum value of $G_s(j\omega)$ is the inverse value of the minimum distance from the point (– 1, 0) to the locus of $G_o(j\omega)$ in the Nyquist plot. The corresponding Bode plot of the sensitivity function is shown in Figure 9.

The sensitivity function offers two advantages over evaluation of the minimum distance on the Nyquist plot. First, it is generally easier to construct the maximum magnitude than it is to find the minimum distance. Indeed, the usual computational method for finding the minimum distance on the Nyquist plot is to find the maximum value of the sensitivity function and then invert it. Second, measurement of the sensitivity function is relatively simple. Referring to Figure 4 b), at a certain point of this closed-loop network we can inject an excitation, $E(s)$, as a harmonic or random signal at an injection point, E, and measure the response signal, V_1, directly behind the injection point. The ratio of these two signals in the frequency domain provides the sensitivity function, G_s, as shown in Equation (5):

$$G_s(s) = \frac{V_1(s)}{E(s)} \tag{5}$$

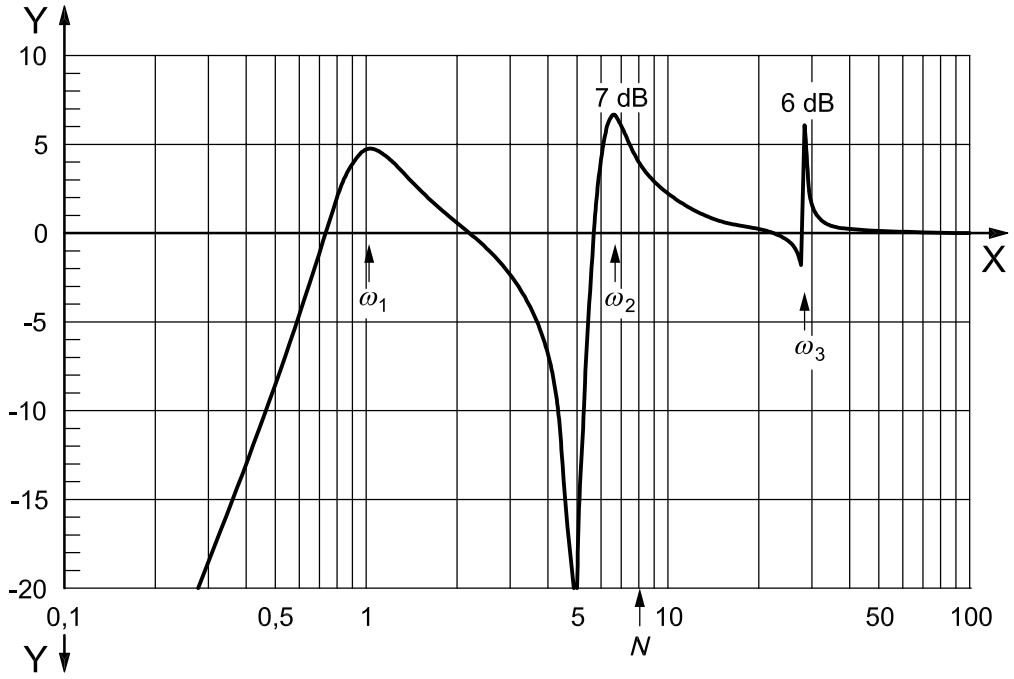

Key

X non-dimensional rotational speed

Y sensitivity gain, expressed in decibels. The decibel (dB) scale is a relative measure: – 20 dB = 0,1; – 10 dB = 0,315; 0 dB = 1; 10 dB = 3,15.

N rated non-dimensional speed

Figure 9 — Bode plot of the sensitivity function, G_s

5 Measurement procedures

5.1 Transfer functions

In the first step of evaluating the stability margin, one of the transfer functions, G_o or G_s, is directly measured with respect to every closed loop. The generalized controller layout is described in Figure 10, where all displacement signals of the five axes are fed into a controller to output the command which determines the magnetic force on the bearings.

NOTE Special controller layouts are shown in Annex A.

In Figure 10, a certain point is selected as the injection point, E, and the open-loop transfer function is measured according to Equation (1), while all other possible injection points are closed. Once the open-loop transfer function, G_o, is measured, the resulting data should be used to form G_s in accordance with Equation (4).

The sensitivity function, G_s, can also be measured directly in accordance with Equation (5).

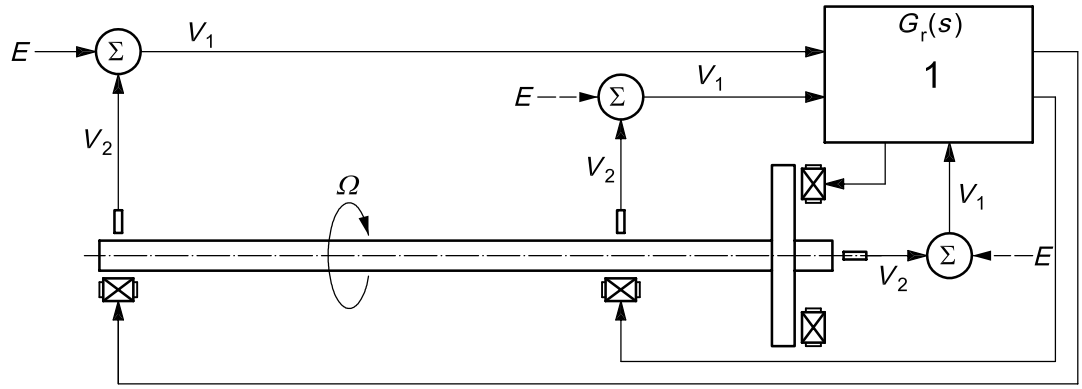

Key

1 central processing unit (CPU)

Figure 10 — Generalized controller layout

5.2 Stability index

When measuring the open-loop transfer function of one control axis, all of the control axes are closed loops. By repeating this measurement step by step for each control axis, a set of the open-loop transfer functions is measured and transferred to sensitivity functions. Otherwise, each sensitivity function is directly measured.

In case of a five-axis control, a total of five sensitivity functions is finally obtained to be evaluated.

The open-loop transfer function or the system's sensitivity function is measured at rotor standstill and/or nominal speed but over the maximum frequency range starting from zero.

In general, there is no need to specify an upper frequency limit since the amplitude of the open-loop transfer function of all technical systems decreases for high frequencies (see Figure 5), rendering both the sensitivity function and the distance margin 1 (0 dB) for all frequencies above a certain limit (see Figures 7 and 9). This automatically ensures stability of the AMB system at very high frequencies. However, in practice for the upper limit, filters are recommended for the signal processing. In this part of ISO 14839, the maximum frequency $f_{\max}$, as given in Equation (6), is set at the larger of

a) three times the rated speed, indicated as 3×, or

b) a maximum frequency of 2 kHz:

$$f_{\max} = \max(3\times, 2\ \text{kHz}) \tag{6}$$

It is noted that, in digitally controlled AMB systems, it is necessary that this maximum frequency be restricted to frequencies below the Shannon frequency (half of the sampling frequency).

From these measured sensitivity functions of each axis in the frequency domain for $0 \leqslant f \leqslant f_{\max}$, the index to be evaluated is obtained from the following relationship with $\omega = 2\pi f$, as given in Equation (7):

$$G_{\text{s,max}} = \max_{i}\left[\max\left|G_{\text{s}}(\text{j}\omega)\right|\right] \quad \text{for } 0 \leqslant f \leqslant f_{\max} \tag{7}$$

where i = 1, ..., the total number of control axes.

Equation (7) generally states that the system's overall rating is determined as the worst rating of any of the transfer functions measured for all five transfer functions individually.

5.3 Measurement conditions

The rotor system is required to behave stably for normal excitations and expected changes of the operating conditions. In-house measurements are required for shipping the equipment, while on-site measurements may be made. The measurements shall be taken under the following conditions:

a) at standstill in-house;

b) at maximum continuous rated speed or nominal power rating in-house or on-site. This location may be decided by mutual agreement between the purchaser and the vendor.

6 Evaluation criteria

6.1 Criterion I

For evaluation of the stability margin, zone limits are given in Table 1. The definition of each stability zone is determined by adapting the guidelines of ISO 7919-1.

— Zone A: The sensitivity functions of newly commissioned machines normally fall within this zone.

— Zone B: Machines with the sensitivity functions within this zone are normally considered acceptable for unrestricted long-term operation.

— Zone C: Machines with the sensitivity functions within this zone are normally considered unsatisfactory for long-term continuous operation. Generally, the machine may be operated for a limited period in this condition until a suitable opportunity arises for remedial action.

— Zone D: The sensitivity functions within this zone are normally considered to be sufficiently severe to cause damage to the machine.

Table 1 — Peak sensitivity at zone limits

Zone	Peak sensitivity	
	Level	Factor
A/B	9,5 dB	3
B/C	12 dB	4
C/D	14 dB	5

As an example of this evaluation, the sensitivity function of Figure 9 is redrawn in the Bode plot of Figure 11 with zone limit values indicated by Table 1. As can be seen from Figure 11, all peak values of the sensitivity function are within zone A.

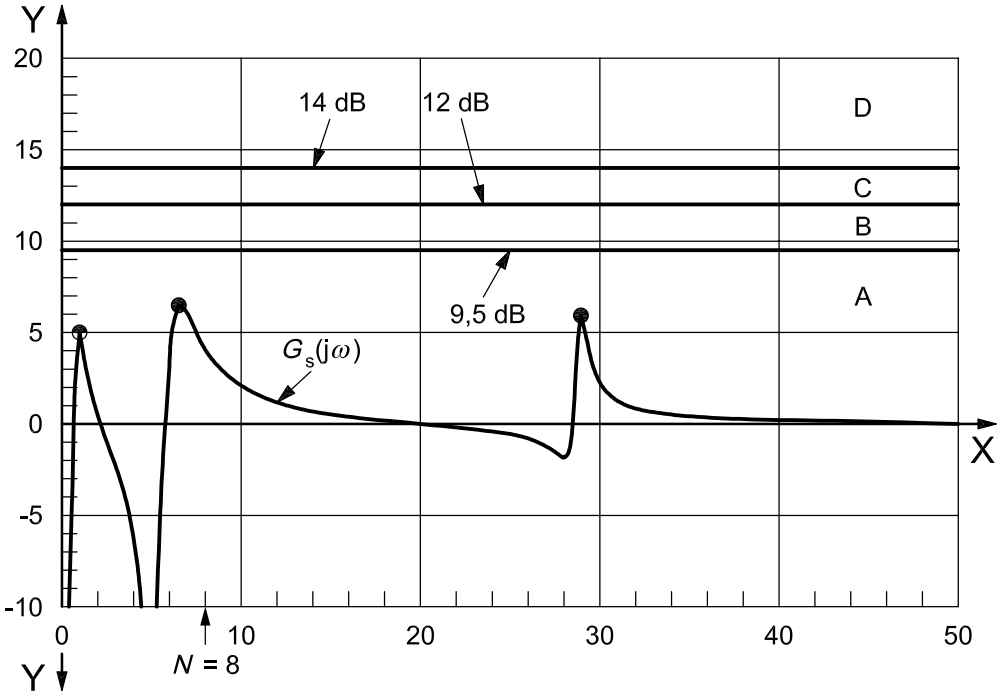

Key

X non-dimensional rotational speed

Y sensitivity gain and zone limits, expressed in decibels

A, B, C, D stability zones

N rated non-dimensional speed

Figure 11 — Evaluation of the stability margin of $G_s(j\omega)$

6.2 Criterion II

This criterion provides an assessment of the change in the stability margins measured periodically from the average values. A significant change in magnitudes of the stability margin can occur that would require remedial action even though zone C of Criterion I has not been reached. Such changes can be progressive with time or instantaneous and can point to incipient damage or some other irregularity.

Criterion II is specified on the basis of the change in magnitude of the stability margin occurring under steady-state operating conditions. When criterion II is applied, it is essential that the measurements being compared are taken under approximately the same machine operating conditions. Significant changes from the normal magnitudes should be regulated to less than 25 % of the upper boundary value of zone B, as defined in Table 1, because a potentially serious fault can be indicated. When a change in the magnitudes is beyond this regulation, the reason for the change shall be determined, and appropriate remediation steps must be planned.

Annex A
(informative)

Case study 1 on evaluation of stability margin

A.1 Test rotor

A test rig and the corresponding rotor is shown in Figures A.1 and A.2. The rotor specification is listed in Table A.1.

The eigen modes and eigen frequencies under free-free conditions are shown in Figure A.3.

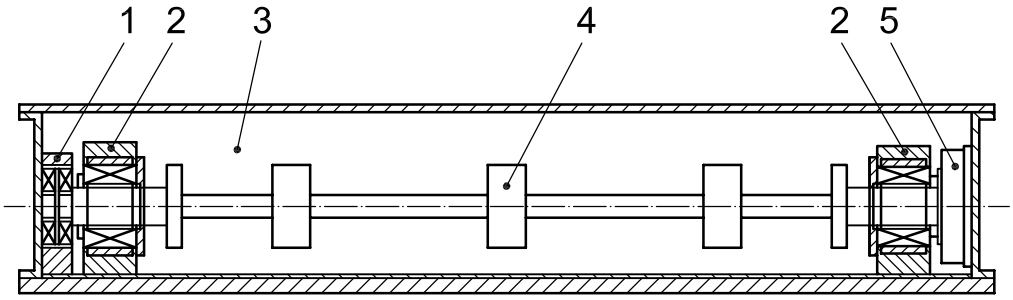

Key

1 thrust AMB
2 radial AMB
3 vacuum chamber
4 flexible rotor
5 motor

Figure A.1 — Test rig

Dimensions in millimetres

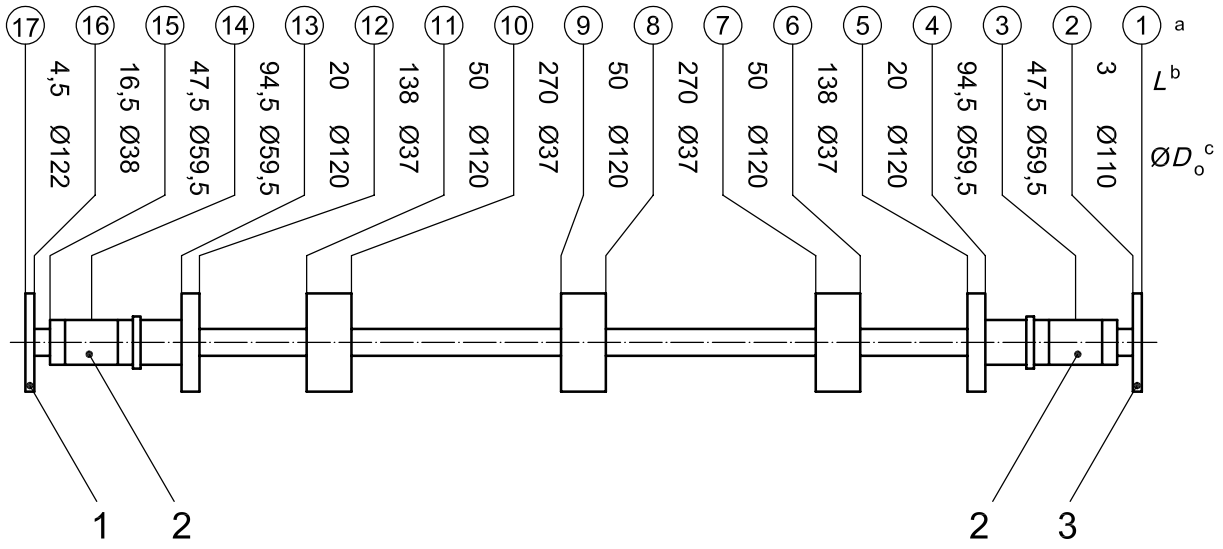

Key

1 thrust AMB rotor

2 radial AMB rotor

3 motor rotor

[a] Nodal points.

[b] Shaft element length, L.

[c] Shaft element diameter, D_0.

Figure A.2 — Structure of the flexible rotor

Table A.1 — Specification of the rotor

Mass	31,4 kg
Shaft diameter	37 mm
Total length	1316 mm
Rated speed	250 rev/s

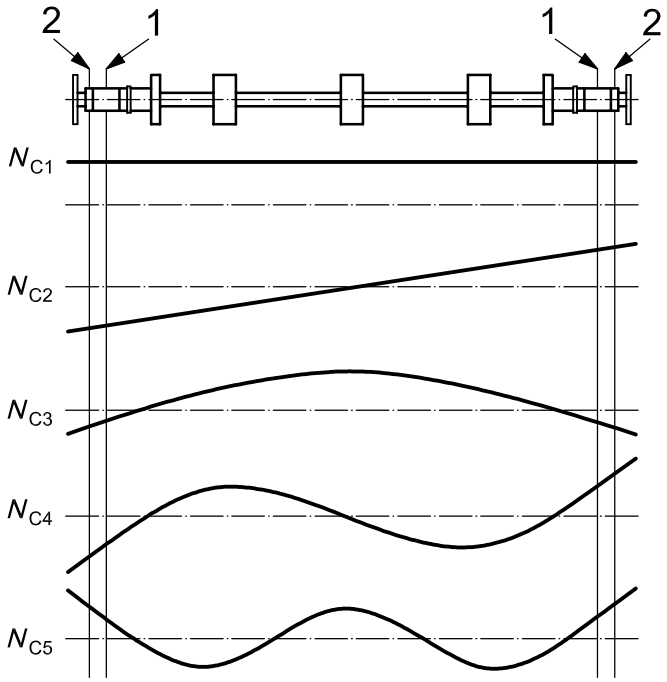

Key

1 plane of AMB

2 plane of sensor

Figure A.3 — Eigen modes and eigen frequencies, N_{Ci}, of the flexible rotor

As shown in the critical speed map in Figure A.4, the intersection between the eigen frequency curve and the AMB stiffness curve indicates the critical speeds of this rotor, noted as N_{Ci}. In the range of operational speeds up to 250 rev/s, four critical speeds are laid out, designated as N_{C1} and N_{C2} indicating the rigid modes and N_{C3} and N_{C4} corresponding to the first two bending modes.

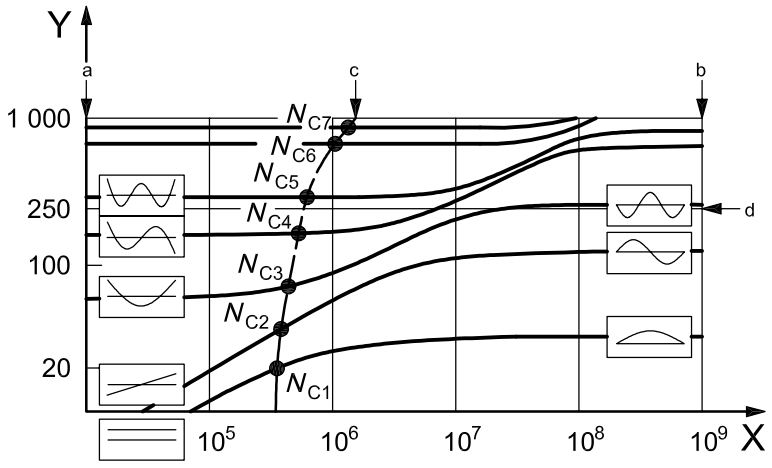

Key

X stiffness, expressed in newtons per metre

Y natural frequency, hertz

a Free-free.

b Pinned-pinned.

c AMB.

d Rated speed.

Figure A.4 — Critical speed map of the flexible rotor

A.2 AMB controllers

Two type of controllers are prepared; “PID” means proportional, integral and differential actions.

a) Type 1: Controller transfer function $G_{\mathrm{r}}(s) = \mathrm{PID} \times \mathrm{PBF}$ (phase bump filter):

The controller layout is decentralized as shown in Figure A.5. Bode plots for the evaluation of the stability margin are shown in Figure A.6.

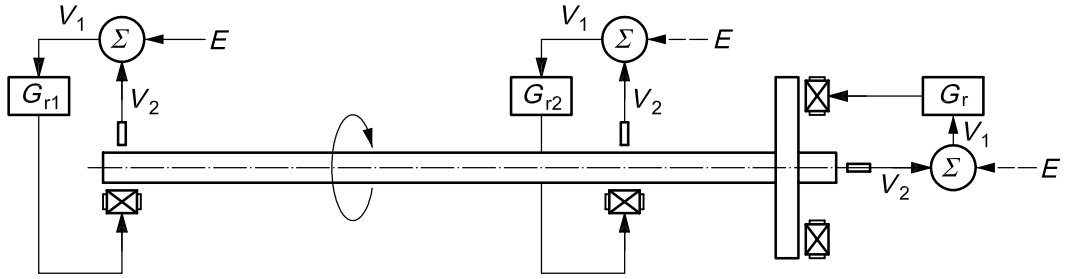

Figure A.5 — Decentralized control

The Bode plot of the open-loop transfer function of the rotor at standstill, G_{o}, was measured as shown in Figure A.6 a) by using a 2-channel FFT analyser. This open-loop transfer function is described in the Nyquist in dB polar diagram in Figure A.6 b), which in Figure A.6 c) shows the behaviour of the shaded range around the frequency 645 Hz corresponding to the N_{C6} mode. The orbit is very close to the critical point (– 1, 0), so that this AMB system is not so stable.

These measured data were rearranged to the sensitivity function, G_{s}, and then described by the Bode plot in Figure A.6 d). The maximum peak of the gain of the sensitivity function is about 14 dB, indicating a poor stability margin. In this manner, the stability margin can be evaluated by the magnitude of the peak of the sensitivity function which, for this example, falls in zone D.

b) Type 2: Controller transfer function $G_{\mathrm{r1}}(s) = \mathrm{PID} \times \mathrm{NF}$ (notch filter);

Controller transfer function $G_{\mathrm{r2}}(s) = \mathrm{PID} \times \mathrm{PSF}$ (phase shift filter):

The controller layout is centralized as shown in Figure A.7, where G_{r1} controls the parallel modes (N_{C1}, N_{C3}, N_{C5}, ...) and G_{r2} controls the tilting modes (N_{C2}, N_{C4}, N_{C6}, ...), respectively. MIMO is a multi input multi output controller. Bode plots for the evaluation of the stability margin are shown in Figures A.8 and A.9.

In the same manner, the open-loop transfer function of the rotor at standstill, G_{o}, was measured as shown in Figure A.8 a), and its Nyquist dB polar diagram as shown in Figures A.8 b) and c) and the sensitivity function G_{s} as shown in Figure A.8 d) were obtained for the tilting mode control, and corresponding drawings in Figure A.9 for the parallel mode control. In this case, the orbit of the open-loop transfer function for the tilting mode control is rather far from the critical point and the peak of the sensitivity function is low except for N_{C2} as shown in the Bode plot of Figure A.8 d). However, the orbit of the open-loop transfer function for the parallel mode control is close to the critical point and the peak of the sensitivity function is high at frequency 300 Hz as shown in the Bode plot of Figure A.9 d). The tilting mode control is within zone C, but the parallel control falls in zone D; consequently this machine is characterized as zone D.

Since the type 2 controller is more stable than the type 1, the rotational test was executed as shown in the vibration magnitude curve of Figure A.10.

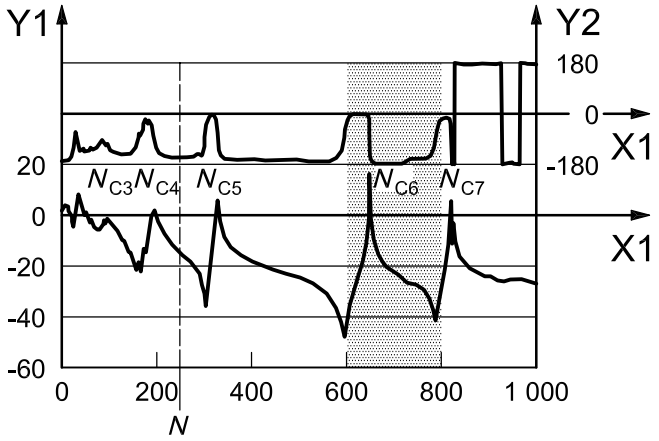

a) Bode plot of the open-loop transfer function, G_o

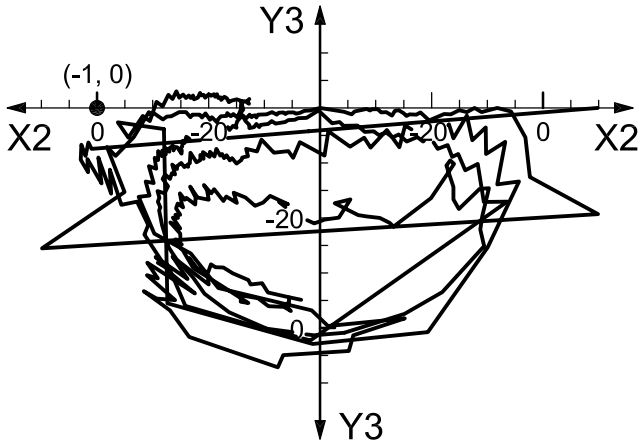

b) Nyquist plot of the open-loop transfer function

Key

X1 frequency, expressed in hertz

X2 decibels

Y1 gain, expressed in decibels. The decibel (dB) scale is a relative measure: − 20 dB = 0,1; − 10 dB = 0,315; 0 dB = 1; 10 dB = 3,15.

Y2 phase, degree

Y3 decibels

N rated speed 250 rev/s

Figure A.6 — Evaluation of the stability margin of the test rotor

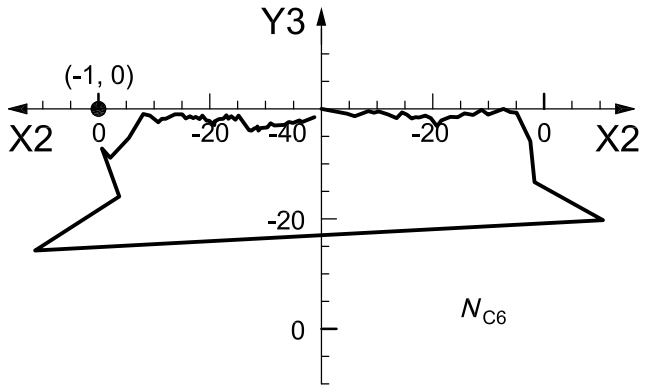

c) Nyquist plot of the shaded range 600 Hz to 800 Hz

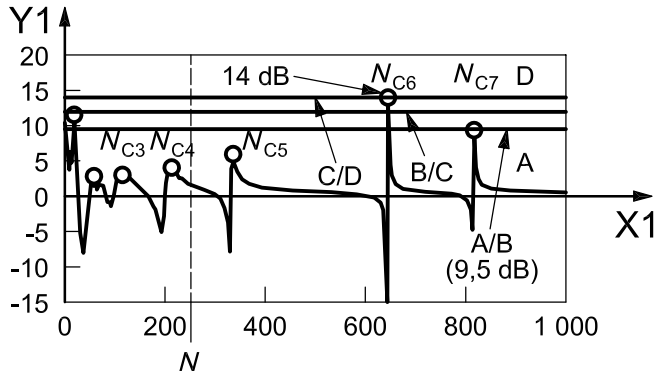

d) Sensitivity function, G_s

Key

X1 frequency, expressed in hertz

X2 decibels

Y1 gain, expressed in decibels. The decibel (dB) scale is a relative measure: − 20 dB = 0,1; − 10 dB = 0,315; 0 dB = 1; 10 dB = 3,15.

Y3 decibels

N rated speed 250 rev/s

A, B, C, D zones; see 6.1

Figure A.6 (*continued*)

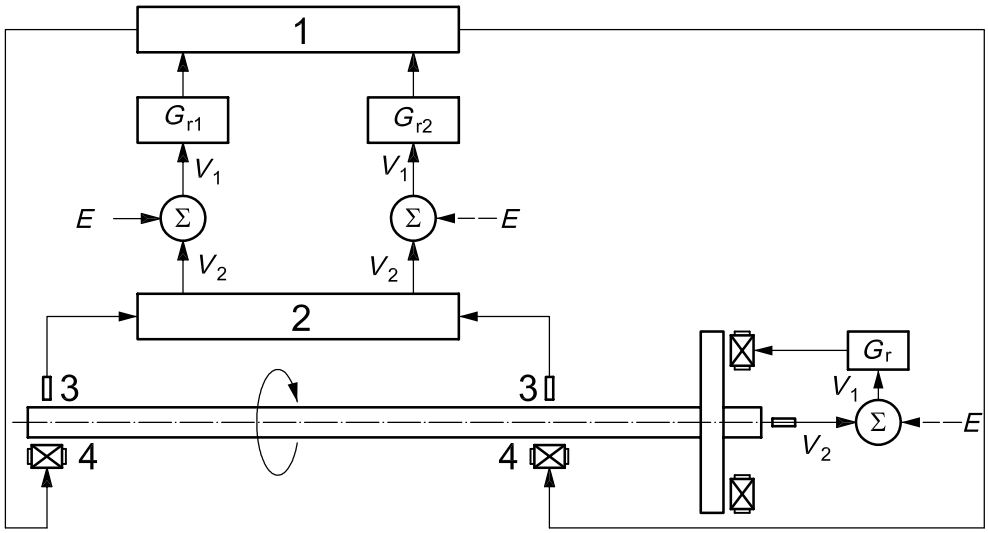

Key

1 recomposition
2 separator
3 sensor
4 AMB

Figure A.7 — Centralized control (MIMO/mode control)

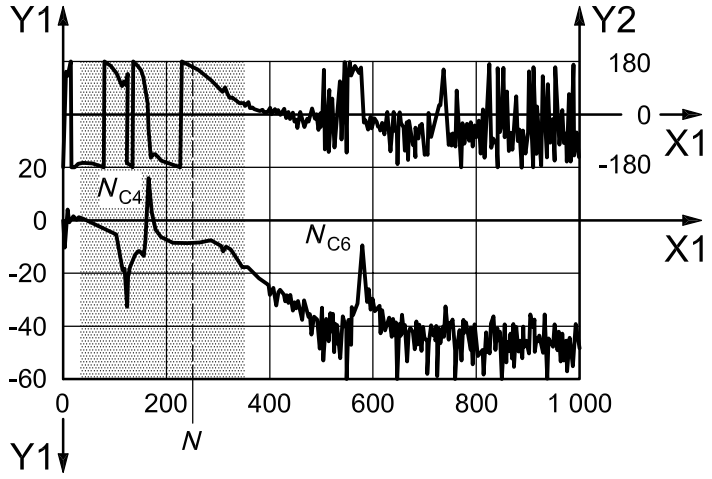

a) Bode plot of the open-loop transfer function, G_o

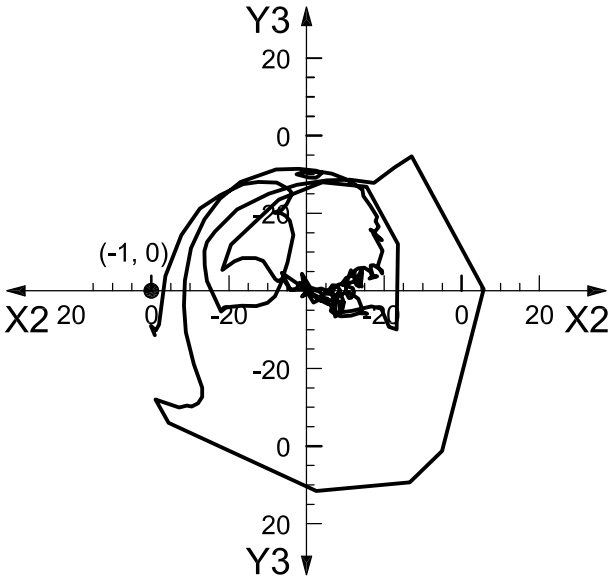

b) Nyquist plot of the open-loop transfer function

Key

X1 frequency, expressed in hertz

X2 decibels

Y1 gain, expressed in decibels. The decibel (dB) scale is a relative measure: − 20 dB = 0,1; − 10 dB = 0,315; 0 dB = 1; 10 dB = 3,15.

Y2 phase, degree

Y3 decibels

N rated speed 250 rev/s

Figure A.8 — Evaluation of the stability margin of the test rotor — Control of tilting modes

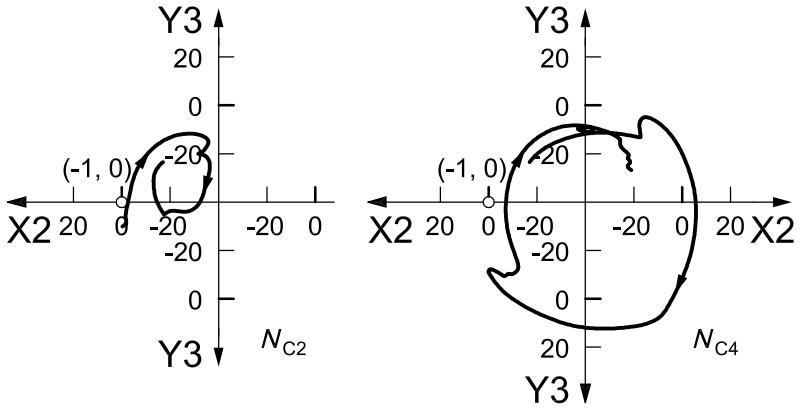

c) Nyquist plot of the shaded range in two sections: left, 30 Hz to 150 Hz; right, 150 Hz to 350 Hz

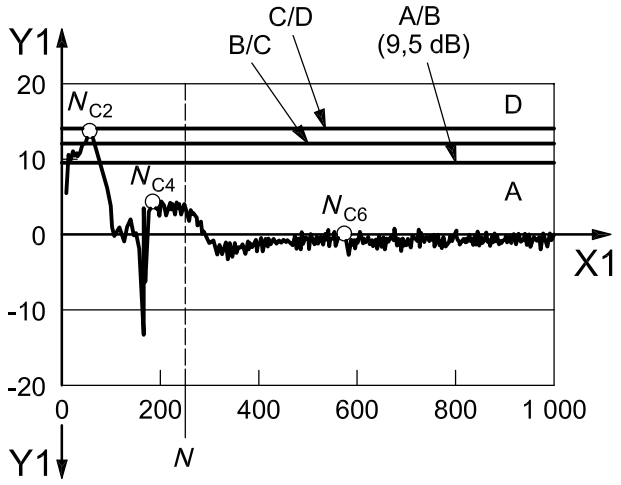

d) Sensitivity function, G_s

Key

X1 frequency, expressed in hertz

X2 decibels

Y1 gain, expressed in decibels. The decibel (dB) scale is a relative measure: – 20 dB = 0,1; – 10 dB = 0,315; 0 dB = 1; 10 dB = 3,15.

Y3 decibels

N rated speed 250 rev/s

A, B, C, D zones; see 6.1

Figure A.8 (*continued*)

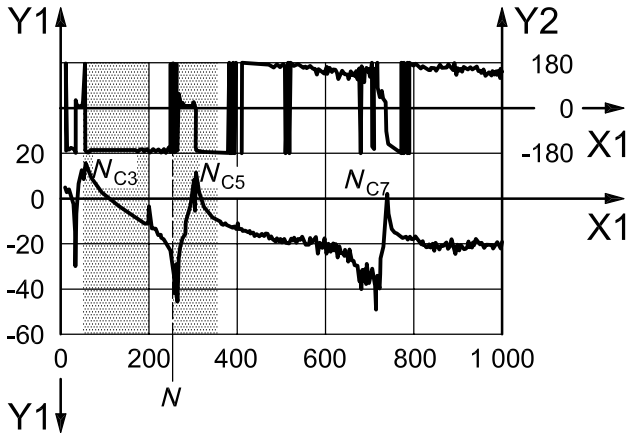

a) Bode plot of the open-loop transfer function, G_o

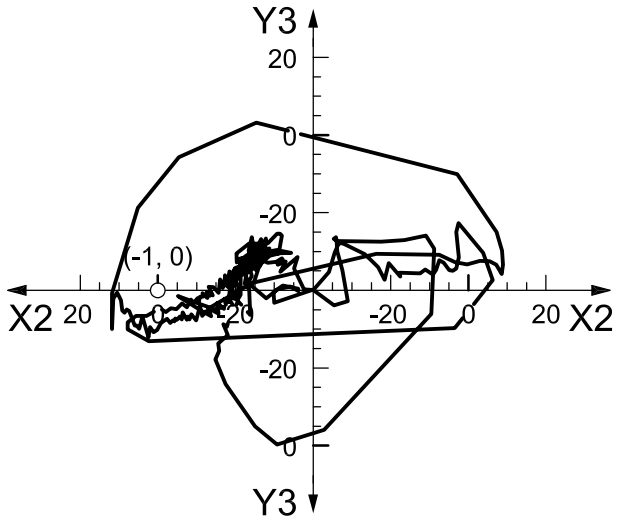

b) Nyquist plot of the open-loop transfer function

Key

X1 frequency, expressed in hertz

X2 decibels

Y1 gain, expressed in decibels. The decibel (dB) scale is a relative measure: − 20 dB = 0,1; − 10 dB = 0,315; 0 dB = 1; 10 dB = 3,15.

Y2 phase, degree

Y3 decibels

N rated speed 250 rev/s

Figure A.9 — Evaluation of the stability margin of the test rotor — Control of parallel modes

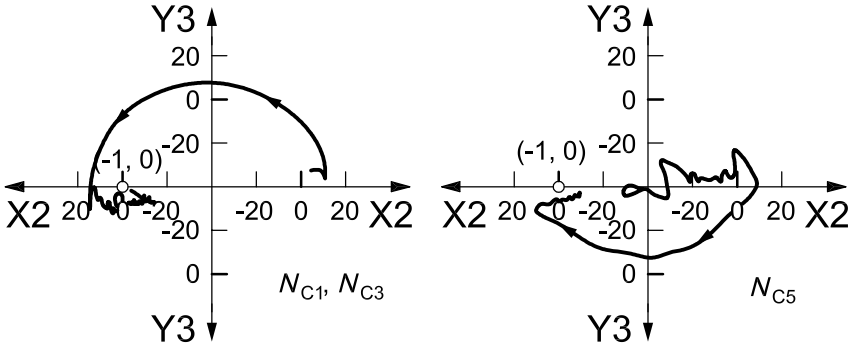

c) Nyquist plot of the shaded ranges: left, 40 Hz to 200 Hz; right, 250 Hz to 350 Hz

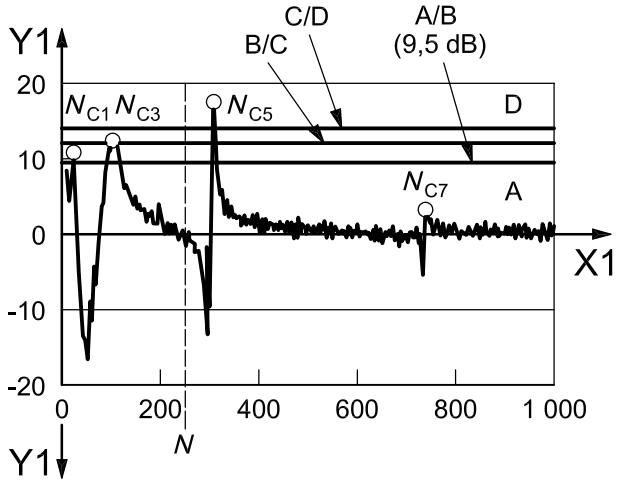

d) Sensitivity function, G_s

Key

X1 frequency, expressed in hertz

X2 decibels

Y1 gain, expressed in decibels. The decibel (dB) scale is a relative measure: – 20 dB = 0,1; – 10 dB = 0,315; 0 dB = 1; 10 dB = 3,15.

Y3 decibels

N rated speed 250 rev/s

A, B, C, D zones; see Table 1

Figure A.9 (*continued*)

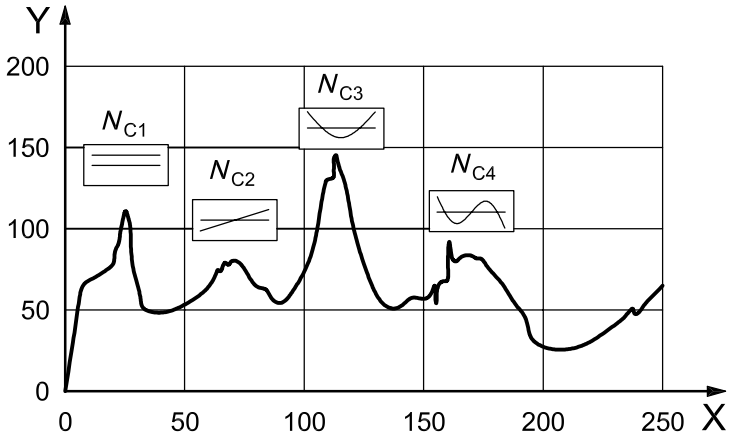

Key

X rotational speed, expressed in revolutions per second

Y peak-to-peak vibration displacement, expressed in micrometres

Figure A.10 — Unbalance vibration response

Annex B
(informative)

Case study 2 on evaluation of stability margin

B.1 AMB compressors

As stated in References [3] and [4], a set of AMB centrifugal compressors was installed at a refinery plant as shown in Figure B.1. This set includes a low-pressure (LP) compressor and a high-pressure (HP) compressor equipped with AMBs. The rotor of the turbine driver is supported by conventional oil-film bearings. A detailed description of these compressor rotors is provided in ISO 14839-2, including eigen frequencies and associated mode shapes, critical speed map, etc. The first eigen frequencies and mode shapes are as follows:

— 1st eigen frequency (translational mode of rigid body): 35 Hz;

— 2nd eigen frequency (tilting mode of rigid body): 82 Hz;

— 3rd eigen frequency (first bending mode under free-free boundary condition): 138 Hz;

— 4th eigen frequency (second bending mode under free-free boundary condition): 276 Hz.

NOTE Rated speed is 10 900 rev/min = 182 Hz.

Dimensions in millimetres

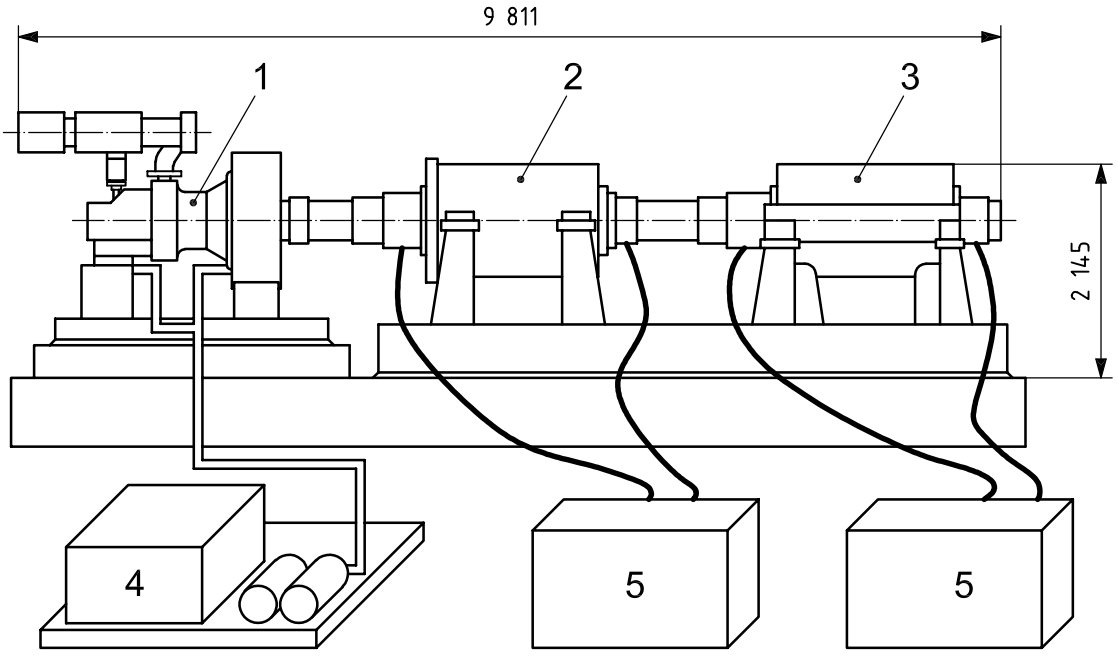

Key
1 turbine
2 high-pressure casing
3 low-pressure casing
4 oil unit
5 electronic control cabinet

Figure B.1 — Arrangement of a centrifugal compressor set with AMBs

B.2 Open-loop transfer function

In this example, the AMB uses side-by-side control. A typical example of an open-loop transfer function was measured as shown in Figure B.2. We can guess that these gain peaks seen in high-frequency domain, 381 Hz, 521 Hz, etc., correspond to eigen frequencies of the shaft bending modes.

B.3 Sensitivity function

This measured open-loop transfer function is rearranged to the sensitivity function in accordance with Equation (4). A Bode plot of this sensitivity function is shown in Figure B.3. Since we can recognize that the value of the highest peak is 3,9 dB (a gain of 1,6), this AMB control system is characterized as zone A according to the zone limit values of Table 1.

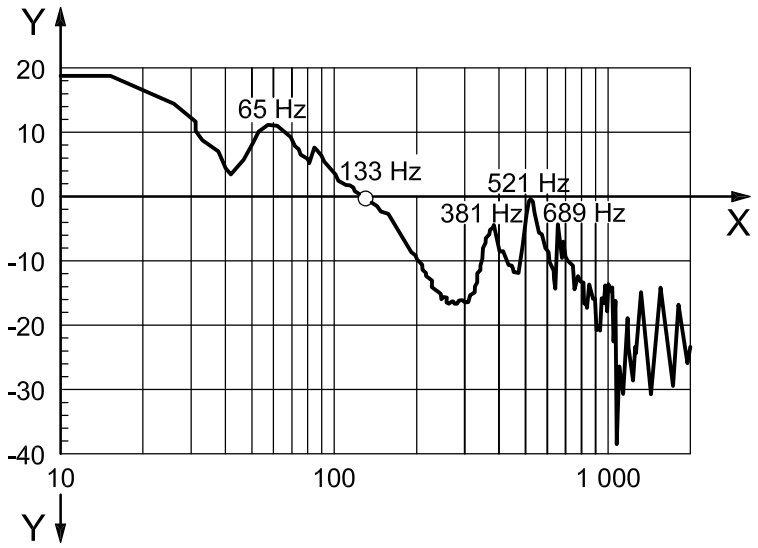

Key

X frequency, expressed in hertz

Y gain, expressed in decibels

Figure B.2 — Bode plot of a typical open-loop transfer function, G_o

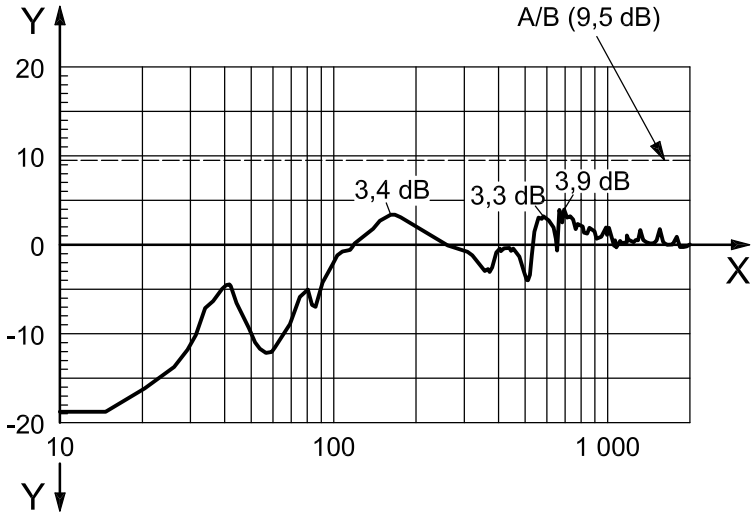

Key

X frequency, expressed in hertz

Y gain, expressed in decibels

A, B zone limit; see Table 1

Figure B.3 — Gain curve of the sensitivity function, G_S

Annex C
(informative)

Field data of stability margin

C.1 AMB test rotor

In 2004, NEDO [1)] organized an international rotational test of an AMB rotor to assess the stability margin, in collaboration with experts collected world-wide. This NEDO test rotor and test rig are shown in Figure C.1 with the rotor specification given in Table C.1. According to calculations of the rotodynamics of the combined rotor and AMB controller, the first system eigen frequencies were predicted as:

— 1st eigen frequency (translational mode of rigid body): 72 Hz;

— 2nd eigen frequency (tilting mode of rigid body): 118 Hz;

— 3rd eigen frequency (first bending mode under free-free boundary condition): 623 Hz;

— 4th eigen frequency (second bending mode under free-free boundary condition): 1 241 Hz.

NOTE Rated speed is 30 000 rev/min = 500 Hz.

Table C.1 — Specification of the NEDO test rotor

Mass	23,76 kg
Moment of inertia, I_d	0,92 kg·m^2
Rated speed	500 rev/s

1) New Energy and Industrial Technology Development Organization, 1-1 Higashi Ikebukuro, 3-chome, Toshima-ku, Tokyo 170-6028, Japan, www.nedo.go.jp.

Dimensions in millimetres

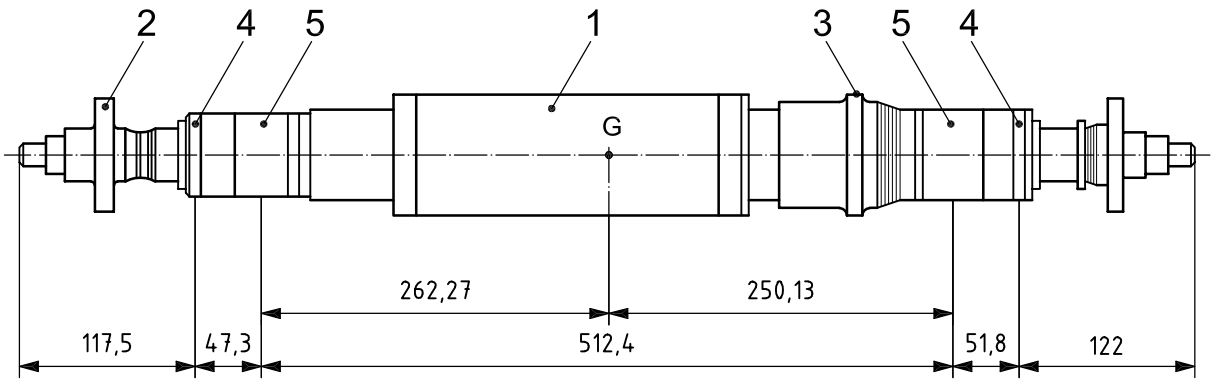

a) Test rotor

b) Test rig

Key

1 motor
2 disc
3 axial AMB
4 sensor
5 radial AMB

Figure C.1 — NEDO test rotor and test rig

C.2 Open-loop transfer function

The AMB is configured as side-by-side control. A typical example of the open-loop transfer function as measured is shown in Figure C.2.

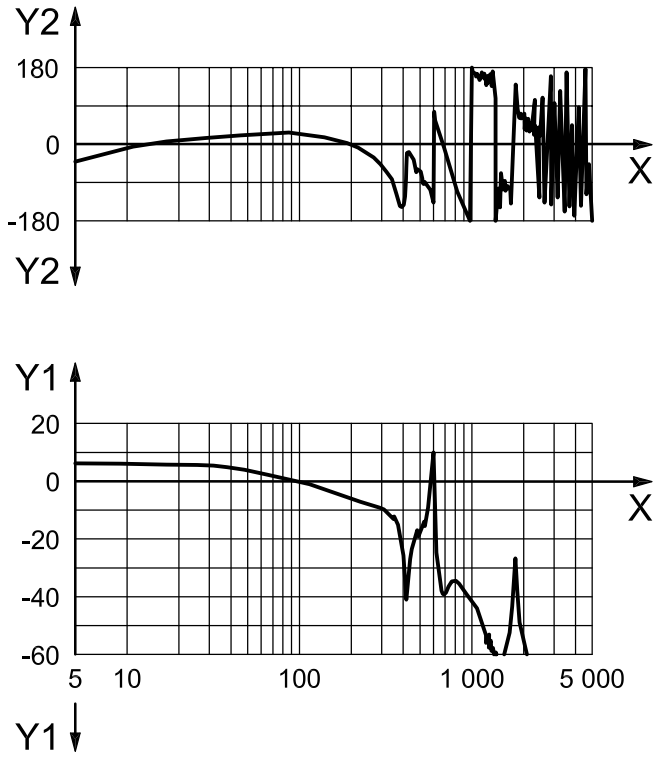

a) Parallel system mode control

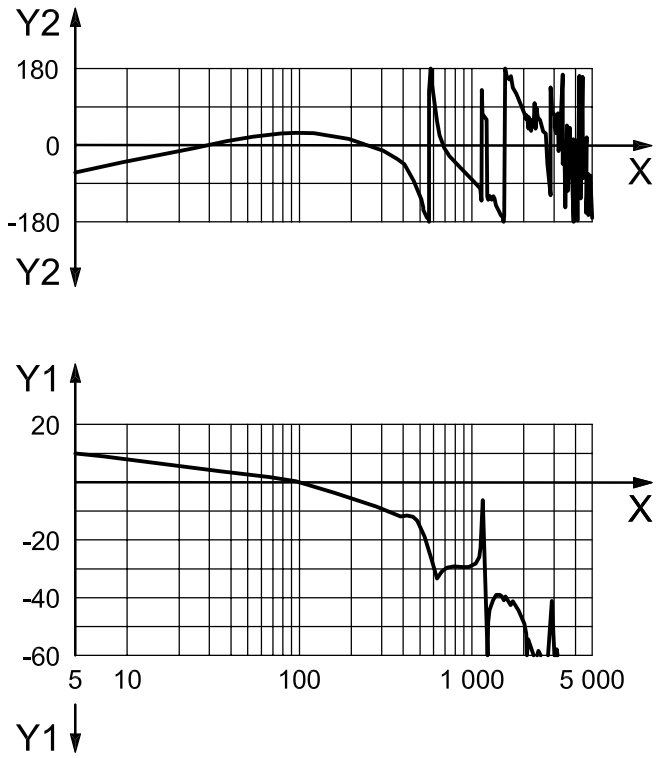

b) Conical system mode control

Key

X frequency, expressed in hertz
Y1 gain, expressed in decibels
Y2 phase, expressed in degrees

Figure C.2 — Bode plot of a typical open-loop transfer function, G_o, of the NEDO test rotor

C.3 Sensitivity function

This measured open-loop transfer function is rearranged to provide the sensitivity function according to Equation (4). The Bode plot of this sensitivity function is shown in Figure C.3.

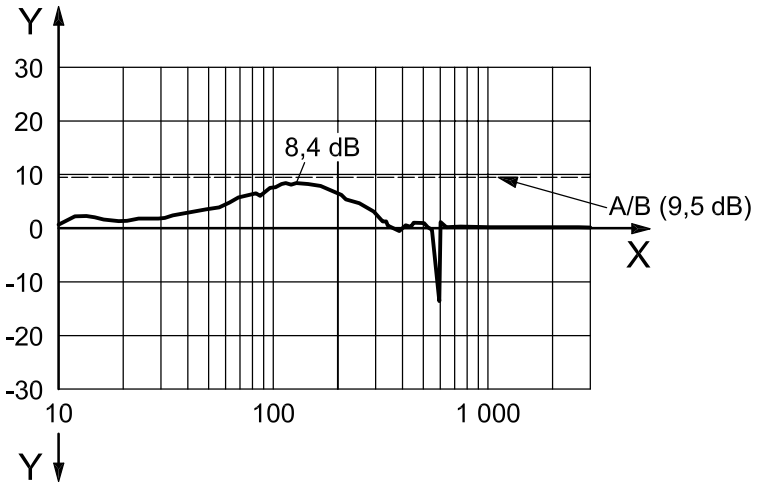

a) Parallel system mode control

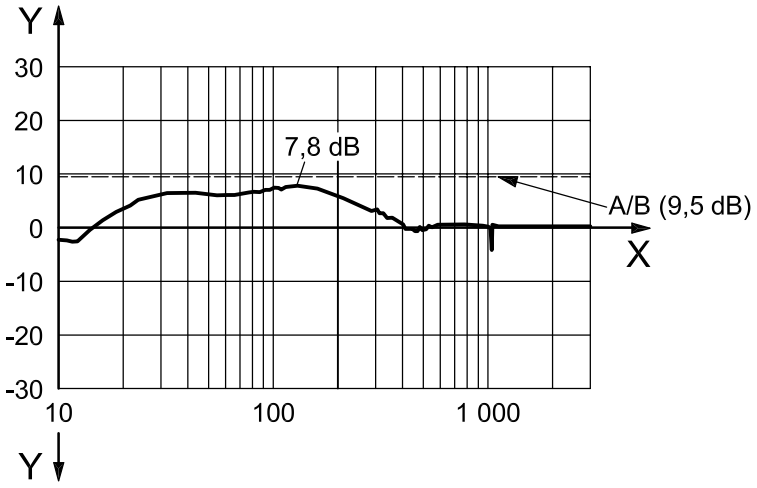

b) Conical system mode control

Key

X frequency, expressed in hertz

Y gain, expressed in decibels

Figure C.3 — Sensitivity function, G_S, of the NEDO test rotor

Annex D
(informative)

Analytical prediction of the system stability

It can be necessary, in the process of design or procurement, to evaluate the expected stability margins of a system prior to its construction. In this case, it is necessary to compute the stability margin, rather than evaluating it. While a full discussion of system modelling for rotors with AMBs is beyond the scope of this part of ISO 14839, some relevant guidelines are given.

First, it is critical that the stability model include the full dynamics of the AMB controller transfer function(s) (including time delay effects), estimates of the sensor bandwidth (represented as low-pass filters in series with the nominal sensor gain), and estimates of the power amplifier bandwidth (also represented as low-pass filters in series with the nominal amplifier gain). These various transfer functions shall not be reduced to an equivalent stiffness and damping by evaluating the transfer function product at the running speed as is commonly done in modelling the stability of fluid-film bearing machines (the so-called synchronously reduced coefficients). The resulting analysis can be expected to be uselessly far from the real stability of the actual machine; indeed, many machines that have very adequate stability margins would be computed to be unstable using such a procedure.

Further, where the rotor has flexible modes within the analysis range, it needs to be modelled as flexible and, in particular, it is necessary to represent the non-collocation of sensors and magnetic actuators accurately in the model. Failure to recognize that the sensors typically do not measure the rotor lateral response at precisely the same axial position at which the magnetic stator/rotor pair acts (see Figure A.3), typically produce analytical results substantially different from the real system's behaviour. This discrepancy gets progressively worse as the mode frequency increases.

Annex E
(informative)

Matrix open loop used for a MIMO system

E.1 "1-cut" open-loop transfer function

The main text of this part of ISO 14839 defines the open-loop transfer function in which one of the five-axis control loops is cut, while the other four loops are closed. This open-loop measurement, based upon single-input and single-output relationship, i.e. in the ISO manner, is conventional when using a two-channel FFT analyser. To implement this part of ISO 14839 for a five-axis AMB system, the measurement of "1-cut" open-loop transfer function is repeated for each control loop. The procedure produces five open-loop transfer functions as given in Equation (E.1):

$$G_{\mathrm{o}1},\ ...,\ G_{\mathrm{o}5} \tag{E.1}$$

These data can then be rearranged to provide five sensitivity functions of the form of Equation (E.2):

$$G_{\mathrm{s}1} = \frac{1}{1+G_{\mathrm{o}1}},\ ...,\ G_{\mathrm{s}5} = \frac{1}{1+G_{\mathrm{o}5}} \tag{E.2}$$

E.2 "N-cut" open-loop transfer function

By using a computer, since it is possible to cut all control loops simultaneously, multiple open-loop transfer functions can be measured. In the case of $N = 5$ control axes, the open-loop transfer function is defined by a matrix form of the relationship between five inputs, $V_{1,i}$, and five outputs, $V_{2,i}$, in the following multiple-input multiple-output (MIMO) manner: $-V_2 = G_{\mathrm{o}} V_1$, as given in Equation (E.3):

$$-\begin{bmatrix} V_{2,1} \\ V_{2,2} \\ V_{2,3} \\ V_{2,4} \\ V_{2,5} \end{bmatrix} = \begin{bmatrix} G_{\mathrm{o}11} & G_{\mathrm{o}12} & G_{\mathrm{o}13} & G_{\mathrm{o}14} & G_{\mathrm{o}15} \\ G_{\mathrm{o}21} & G_{\mathrm{o}22} & G_{\mathrm{o}23} & G_{\mathrm{o}24} & G_{\mathrm{o}25} \\ G_{\mathrm{o}31} & G_{\mathrm{o}32} & G_{\mathrm{o}33} & G_{\mathrm{o}34} & G_{\mathrm{o}35} \\ G_{\mathrm{o}41} & G_{\mathrm{o}42} & G_{\mathrm{o}43} & G_{\mathrm{o}44} & G_{\mathrm{o}45} \\ G_{\mathrm{o}51} & G_{\mathrm{o}52} & G_{\mathrm{o}53} & G_{\mathrm{o}54} & G_{\mathrm{o}55} \end{bmatrix} \begin{bmatrix} V_{1,1} \\ V_{1,2} \\ V_{1,3} \\ V_{1,4} \\ V_{1,5} \end{bmatrix} \tag{E.3}$$

This MIMO control system is drawn in Figure E.1. Note that this open-loop transfer matrix can also be measured for an N-axis machine, but it is necessary to measure all signals, $V_{1,i}$ and $V_{2,i}$, simultaneously.

The corresponding sensitivity function is defined in a similar matrix form, as given in Equation (E.4):

$$G_{\mathrm{s}} = (\mathbf{1}+G_{\mathrm{o}})^{-1} = \begin{bmatrix} G_{\mathrm{s}11} & G_{\mathrm{s}12} & G_{\mathrm{s}13} & G_{\mathrm{s}14} & G_{\mathrm{s}15} \\ G_{\mathrm{s}21} & G_{\mathrm{s}22} & G_{\mathrm{s}23} & G_{\mathrm{s}24} & G_{\mathrm{s}25} \\ G_{\mathrm{s}31} & G_{\mathrm{s}32} & G_{\mathrm{s}33} & G_{\mathrm{s}34} & G_{\mathrm{s}35} \\ G_{\mathrm{s}41} & G_{\mathrm{s}42} & G_{\mathrm{s}43} & G_{\mathrm{s}44} & G_{\mathrm{s}45} \\ G_{\mathrm{s}51} & G_{\mathrm{s}52} & G_{\mathrm{s}53} & G_{\mathrm{s}54} & G_{\mathrm{s}55} \end{bmatrix} \tag{E.4}$$

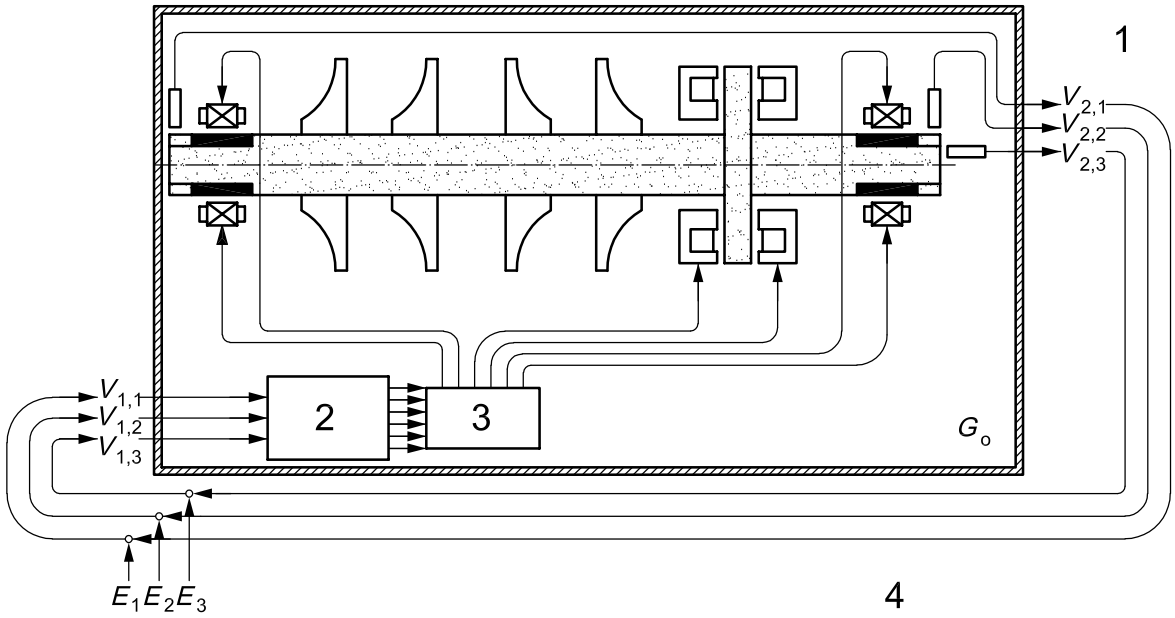

Key

1 signals from position sensors
2 controller
3 power amplifiers
4 normal operating feedback path

Figure E.1 — Open-loop transfer functions of a MIMO system

E.3 Relationship between “1-cut” and "N-cut" procedures

For example, when we calculate the “1-cut” open-loop transfer function of channel 1, we solve Equation (E.3) to obtain the ratio of “1-cut”, i.e. $G_{o1} = V_{2,1} / V_{1,1}$, under the assumption of the closed loop of all other channels, i.e. $V_{2,2} = V_{1,2}, V_{2,3} = V_{1,3}, V_{2,4} = V_{1,4}, V_{2,5} = V_{1,5}$. Therefore, compared with Equations (E.1) and (E.3), these open-loop transfer functions are different, as given in Equation (E.5):

$$G_{ok} \neq G_{okk} \text{ for } k = 1, \ldots, 5 \tag{E.5}$$

It is noted that these measured open-loop transfer functions are not the same, although both are referred to as “open-loop transfer functions”.

However, each diagonal element of the matrix sensitivity function of Equation (E.4) is the same as the corresponding conventional sensitivity function of Equation (E.2), as given in Equation (E.6):

$$G_{sk} = G_{skk} \text{ for } k = 1, \ldots, 5 \tag{E.6}$$

As a result, this part of ISO 14839 states the evaluation of stability margin based upon the sensitivity transfer function, G_{sk}, obtained by “1-cut” conventional open-loop transfer functions measured by using FFT analyser. In the case of “N-cut” matrix open-loop transfer functions measured by using a computer, the diagonal elements, G_{skk}, should be equivalently replaced as the performance index to be subject to this part of ISO 14839.

Bibliography

[1] ISO 7919 (all parts), *Mechanical vibration of non-reciprocating machines — Measurements on rotating shafts and evaluation criteria*

[2] ISO 11342, *Mechanical vibration — Methods and criteria for the mechanical balancing of flexible rotors*

[3] FUKUSHIMA, Y. *et al*. Totally oil-free centrifugal compressor in oil refinery service, *Proceedings of Advancement in Bearing and Seal Technology*, Calgary, Canada, 1994, pp. 18.1-18.36

[4] MATSUSHITA, O., KANEMITSU, Y., AZUMA, T. AND FUKUSHIMA, Y. Vibration criteria considered from case studies of active magnetic bearing equipped rotating machines, *International Journal of Rotating Machinery*, **6**(1), 2000, pp. 66-78

[5] ISO 14839-2, *Mechanical vibration — Vibration of rotating machinery equipped with active magnetic bearings — Part 2: Evaluation of vibration*

ICS 17.160

Price based on 35 pages